

Simulating *Gaia* performances on white dwarfs

Santiago Torres^{1,2}, Enrique García–Berro^{1,2}, Jordi Isern^{2,3} and Francesca Figueras^{2,4}

¹*Departament de Física Aplicada, Escola Politècnica Superior de Castelldefels, Universitat Politècnica de Catalunya, Avda. del Canal Olímpic s/n, 08860 Castelldefels, Spain*

²*Institute for Space Studies of Catalonia, c/Gran Capità 2–4, Edif. Nexus 104, 08034 Barcelona, Spain*

³*Institut de Ciències de l’Espai, C.S.I.C., Campus UAB, Facultat de Ciències, Torre C-5, 08193 Bellaterra, Spain*

⁴*Departament d’Astronomia i Meteorologia, Universitat de Barcelona, Facultat de Física, Martí i Franquès 1, 08028 Barcelona, Spain*

4 December 2018

ABSTRACT

One of the most promising space missions of ESA is the astrometric satellite *Gaia*, which will provide very precise astrometry and multicolour photometry, for all 1.3 billion objects to $V \sim 20$, and radial velocities with accuracies of a few km s^{-1} for most stars brighter than $V \sim 17$. Consequently, full homogeneous six-dimensional phase-space information for a huge number of stars will become available. Our Monte Carlo simulator has been used to estimate the number of white dwarfs potentially observable by *Gaia*. From this we assess which would be the white dwarf luminosity functions which *Gaia* will obtain and discuss in depth the scientific returns of *Gaia* in the specific field of white dwarf populations. Scientific attainable goals include, among others, a reliable determination of the age of the Galactic disk, a better knowledge of the halo of the Milky Way and the reconstruction of the star formation history of the Galactic disk. Our results also demonstrate the potential impact of a mission like *Gaia* in the current understanding of the white dwarf cooling theory.

Key words: stars: white dwarfs — stars: luminosity function, mass function — Galaxy: stellar content — Galaxy: dark matter — Galaxy: structure — Galaxy: halo

1 INTRODUCTION

Gaia is an ambitious space mission (Perryman et al. 2001), adopted within the scientific programme of the European Space Agency (ESA) in October 2000 — see, for instance, <http://astro.estec.esa.nl/GAIA/>. It aims to measure the positions and proper motions of an extremely large number of objects with unprecedented accuracy. As a result, a three-dimensional map of the positions (and velocities) of a sizeable fraction of the stars of our Galaxy will be obtained, as well as solar system objects and extragalactic sources. The precision of the angular measurements will be of about $3 \mu\text{as}$ at 12^{mag} , $10 \mu\text{as}$ at 15^{mag} , and degrading to $200 \mu\text{as}$ at 20^{mag} . The satellite will continuously scan the sky, allowing for astrometric measurements on the so-called Astrometric Field (AF), and for broad-band photometry on a Broad Band Photometer (BBP). Full sky coverage will be possible because of the spin of the satellite around its own axis, which itself precesses at a fixed angle with respect to the Sun. Spectra and medium-band photometry will also be obtained for selected sources on the SPECTRO and MBP instruments, respectively, from which the radial velocity of the detected sources will be obtained. This will lead to the most complete and accurate map of the stars of our Galaxy.

Gaia will be the successor of the astrometric satellite *Hipparcos*, which was operative from 1989 to 1993. The sci-

entific program of *Hipparcos* was more modest than that of *Gaia* since it measured the positions and proper motions of only 10^5 rather than $\sim 10^9$ Galactic objects. Moreover, *Hipparcos* operated on the basis of an input catalogue. Instead, *Gaia* will determine its own targets. In order to do so, *Gaia* will use a series of sky mappers and a sophisticated on-board detection and selection algorithm to produce a list of targets to be subsequently followed in the AF, the MBP, the BBP and the SPECTRO instruments. Finally, the scientific products of *Hipparcos* were released only when the mission was complete, whereas some of the scientific data that *Gaia* will collect will be partially released during the 5 yr duration of the mission.

White dwarfs are the end-product of the evolution of low- and intermediate-mass stars. Thus, they preserve important clues about the formation and evolution of our Galaxy. This information can be retrieved by studying their observed mass, kinematic and luminosity distributions, provided that we have good structural and evolutionary models for the progenitors of white dwarfs and for the white dwarf themselves. In particular, the fundamental tool to analyze the properties of the white dwarf population as a whole is the white dwarf luminosity function, which has been consistently used to obtain estimates of the age of the Galactic disk (Winget et al. 1987; García–Berro et al. 1988; Hernanz

et al. 1994; Richer et al. 2000) and the past history of the Galactic star formation rate (Noh & Scalo 1990; Díaz–Pinto et al. 1994; Isern et al. 1995; Isern et al. 2001). Although the situation for the disk white dwarf population seems to be relatively clear and well understood, this is not the case for the halo white dwarf population. The discovery of microlenses towards the Large Magellanic Cloud (Alcock et al. 1996, Alcock et al. 2000; Lasserre et al. 2001) generated a large controversy about the possibility that white dwarfs could be responsible for these microlensing events and, thus, could provide a significant contribution to the mass budget of our Galactic halo. In both cases *Gaia* will potentially have a large impact. Consequently, it is desirable to foresee which would be the scientific returns of *Gaia* in the field of white dwarfs.

In this paper we assess the number of white dwarfs potentially observable by *Gaia*. In doing this our Monte Carlo simulator (García–Berro et al. 1999; Torres et al. 1998) has been used. Our results show which could be the impact of a mission like *Gaia* in the current understanding of the Galactic white dwarf population. This work is organized as follows. In §2 a brief description of our Monte Carlo simulator is given. Section 3 is devoted to analyze the results of our simulations, including the completeness of the samples of disk and halo white dwarfs, and the accuracy of the astrometric determinations of both samples. In this section a study of the expected disk and halo white dwarf luminosity functions which *Gaia* will presumably obtain is also done, and from this the scientific attainable goals are discussed in depth. Finally, §4 is devoted to summarize our conclusions and to discuss the results obtained here.

2 THE MONTE CARLO SIMULATOR

Since our Monte Carlo simulator has been thoroughly described in previous papers (García–Berro et al. 1999; García–Berro et al. 2004) we will only summarize here the most important inputs. As in any Monte Carlo simulation one of the most important ingredients is a random number generator. We have used a pseudo-random number generator algorithm (James 1990) which provides a uniform probability density within the interval (0, 1) and ensures a repetition period of $\gtrsim 10^{18}$, which is virtually infinite for practical simulations. When gaussian probability functions are needed we have used the Box-Muller algorithm as described in Press et al. (1986). Moreover, each one of the Monte Carlo simulations discussed below consists of an ensemble of 40 independent realizations of the synthetic white dwarf population, for which the average of any observational quantity along with its corresponding standard deviation were computed. Here the standard deviation means the ensemble mean of the sample dispersions for a typical sample.

In our simulations we have adopted a disk age ranging from 8 to 13 Gyr (see §3.3). White dwarfs have been distributed according to an exponential density law with a scale length $L = 3.5$ kpc in Galactocentric radius. A standard initial mass function (Scalo 1998) and a constant volumetric star formation rate were adopted, although in section §3.3 we also explore other star formation rates. The velocities have been drawn from normal laws:

$$\begin{aligned} n(U) &\propto e^{-(U-U'_0)^2/\sigma_U^2} \\ n(V) &\propto e^{-(V-V'_0)^2/\sigma_V^2} \\ n(W) &\propto e^{-(W-W'_0)^2/\sigma_W^2} \end{aligned} \quad (1)$$

where (U'_0, V'_0, W'_0) take into account the differential rotation of the disk (Ogorodnikov 1965), and derive from the peculiar velocity $(U_\odot, V_\odot, W_\odot)$ of the sun with respect to the local standard of rest, for which we have adopted the value $(10, 5, 7)$ km s $^{-1}$ (Dehnen & Binney 1997). The three velocity dispersions $(\sigma_U, \sigma_V, \sigma_W)$, and the lag velocity, V_0 , depend on the adopted scale height (Mihalas & Binney 1981):

$$\begin{aligned} U_0 &= 0 \\ V_0 &= -\sigma_U^2/120 \\ W_0 &= 0 \end{aligned} \quad (2)$$

$$\begin{aligned} \sigma_V^2/\sigma_U^2 &= 0.32 + 1.67 \cdot 10^{-5} \sigma_U^2 \\ \sigma_W^2/\sigma_U^2 &= 0.50 \\ \sigma_W^2 &= 1.53 \cdot 10^3 H_p, \end{aligned} \quad (3)$$

where the units are, respectively, kpc and km s $^{-1}$. We have used $H_p = 500$ pc. A standard model of Galactic absorption has been used as well (Hakkila et al. 1997).

In the model the halo is assumed to be formed 14 Gyr ago in an intense burst of star formation of duration 1 Gyr (see, however, §3.4 below). The synthetic white dwarfs have been distributed according to a typical isothermal, spherically symmetric halo:

$$\rho(r) = \rho_0 \frac{a^2 + R_\odot^2}{a^2 + r^2} \quad (4)$$

where $a \approx 5$ kpc is the core radius, ρ_0 is the local halo density and $R_\odot = 8.5$ kpc is the Galactocentric distance of the Sun. A standard initial mass function was adopted as well. The velocities of halo stars were randomly drawn from normal distributions (Binney & Tremaine 1987):

$$f(v_r, v_t) = \frac{1}{(2\pi)^{3/2}} \frac{1}{\sigma_r \sigma_t^2} \exp \left[-\frac{1}{2} \left(\frac{v_r^2}{\sigma_r^2} + \frac{v_t^2}{\sigma_t^2} \right) \right] \quad (5)$$

where σ_r and σ_t — the radial and the tangential velocity dispersion, respectively — are related by the following expression:

$$\sigma_t^2 = \frac{V_c^2}{2} + \left[1 - \frac{r^2}{a^2 + r^2} \right] \sigma_r^2 + \frac{r}{2} \frac{d(\sigma_r^2)}{dr} \quad (6)$$

which, to a first approximation, leads to $\sigma_r = \sigma_t = V_c/\sqrt{2}$ — see, for instance, Binney & Tremaine (1987). For the calculations reported here we have adopted a circular velocity $V_c = 220$ km/s. From these velocities we obtain the heliocentric velocities by adding the velocity of the LSR $v_{\text{LSR}} = -220$ km/s and the peculiar velocity of the sun. The velocity dispersions σ_r and σ_t are those determined by Marković & Sommer–Larsen (1996). In particular, the radial velocity dispersion is given by:

$$\sigma_r^2 = \sigma_0^2 + \sigma_+^2 \left[\frac{1}{2} - \frac{1}{\pi} \arctan \left(\frac{r - r_0}{l} \right) \right] \quad (7)$$

whereas the tangential dispersion is given by:

$$\sigma_t^2 = \frac{1}{2}V_c^2 - \left(\frac{\gamma}{2} - 1\right)\sigma_r^2 + \frac{r}{2}\frac{d\sigma_r^2}{dr} \quad (8)$$

where

$$r\frac{d\sigma_r^2}{dr} = -\frac{1}{\pi}\frac{r}{l}\frac{\sigma_+^2}{1 + [(r - r_0)/l]^2} \quad (9)$$

The values of the constants are, respectively $\sigma_0 = 80 \text{ km s}^{-1}$, $\sigma_+ = 145 \text{ km s}^{-1}$, $r_0 = 10.5 \text{ kpc}$ and $l = 5.5 \text{ kpc}$,

The procedure to obtain the synthetic stars is the following. First, we randomly choose the three-dimensional coordinates of each star of the sample according to the adopted density laws. Afterwards we draw another pseudo-random number in order to obtain the main sequence mass of each star, according to the initial mass function. Once the mass of the progenitor of the white dwarf is known we randomly choose the time at which each star was born, according to the star formation rate of the population under study. Given the age of the corresponding population and the main sequence lifetime as a function of the mass in the main sequence (Iben & Laughlin 1989) we know which stars have lived long enough to become white dwarfs, and given a set of fully evolutionary cooling sequences for several white dwarf masses (Salaris et al. 2000) — which reproduce the so-called “blue hook” of hydrogen-rich (DA) white dwarfs — and the initial to final mass relationship (Iben & Laughlin 1989), their present day luminosities and magnitudes. The magnitude is then corrected for Galactic extinction and reddening and converted to the instrumental magnitude of *Gaia*, G , which is related to the standard colours ($V, V - I$) by the expression (Perryman 2002):

$$G - V = -0.00544 - 0.36919(V - I) - 0.09727(V - I)^2 + 0.00372(V - I)^3 \quad (10)$$

The typical errors in parallax depend on the magnitude (Perryman 2002) and are computed using the following fitting function:

$$\sigma_\pi \simeq \sqrt{7 + 105z + 1.3z^2 + 6 \cdot 10^{-10}z^6} \times [0.96 + 0.04(V - I)] \quad (11)$$

where σ_π is given in μas and $\log z = 0.4(G - 15)$. The errors in parallax, σ_π , and proper motion, σ_μ , in $\mu\text{as yr}^{-1}$, are related by $\sigma_\mu = 0.75\sigma_\pi$ (Perryman 2002).

In this way we end up with all the relevant information necessary to assess the performance of *Gaia*. It is important to mention at this point that since the number of synthetic stars necessary to simulate the whole Galaxy is prohibitively large we have only determined the number of white dwarfs that could eventually be detected within 400 pc of the sun. The number density of white dwarfs in this sphere of radius 400 pc was normalized to the local observed density of either disk (Oswalt et al. 1996) or halo white dwarfs (Torres et al. 1998), depending on the population under study. Additionally, we have computed the total number of white dwarfs in a small window of $1^\circ \times 1^\circ$ (termed a “pencil beam”) for each of the three directions shown in figure 1. Since the direction $l = 0^\circ$, $b = 0^\circ$ corresponds to the direction in the Galactic plane for which Galactic extinction, statistically speaking, is expected to be a maximum we have also computed the total number of white dwarfs in the direction $l = 180^\circ$, $b = 0^\circ$,

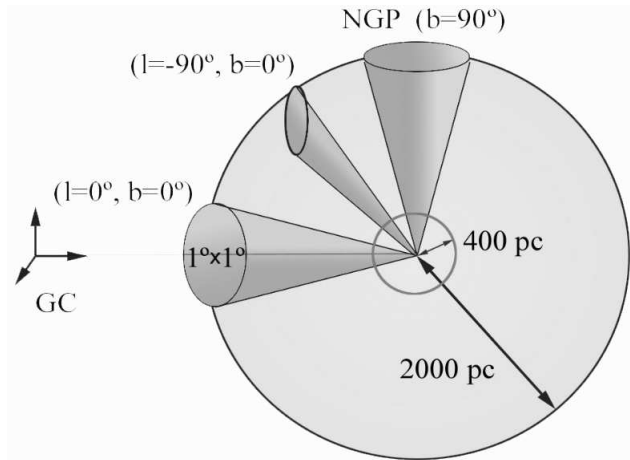


Figure 1. The adopted geometry for the Monte Carlo simulations.

which corresponds to a minimum extinction on the Galactic plane. Each of these pencil beams has a depth of 2000 pc and is again normalized to the observed local density of white dwarfs. Obviously, only the brightest white dwarfs will be seen at very large distances. After doing this we average our results over the corresponding octant and we repeat the procedure for the rest of octants. Finally we average our results over the whole sky in order to obtain an estimate of the total number of white dwarfs within 2 kpc of the sun accessible to *Gaia*.

3 RESULTS

3.1 Expected number of disk and halo white dwarfs

The total number of disk white dwarfs along the three above mentioned pencil beams of the first octant and the total number of white dwarfs accessible to *Gaia* are shown in table 1 for different limiting magnitudes, between $G_{\text{lim}} = 20$ and 21, since the real limiting magnitude of *Gaia* will depend on the specific technical design. Also, in figure 2 we show the distribution of white dwarfs in a typical realization of the Monte Carlo simulations, as a function of their apparent G magnitude for each one of the three pencil beams considered here, and $G_{\text{lim}} = 20$. The shaded histograms correspond to the case in which Galactic extinction has been taken into account, whereas the dashed histograms correspond to the case in which Galactic extinction was disregarded. As can be seen in figure 2 the effects of Galactic extinction are quite evident. Note as well that the number of white dwarfs potentially observable by *Gaia* decreases considerably when Galactic extinction is taken into account.

In figure 3 we show the distribution in the number of disk white dwarfs detected by *Gaia* as a function of their absolute magnitude, according to their errors in parallax, for 100, 200, 300 and 400 pc and $G_{\text{lim}} = 20$. Fig. 3 shows that *Gaia* will detect faint white dwarfs up to considerable distances. It is noticeable that *Gaia* will detect white dwarfs

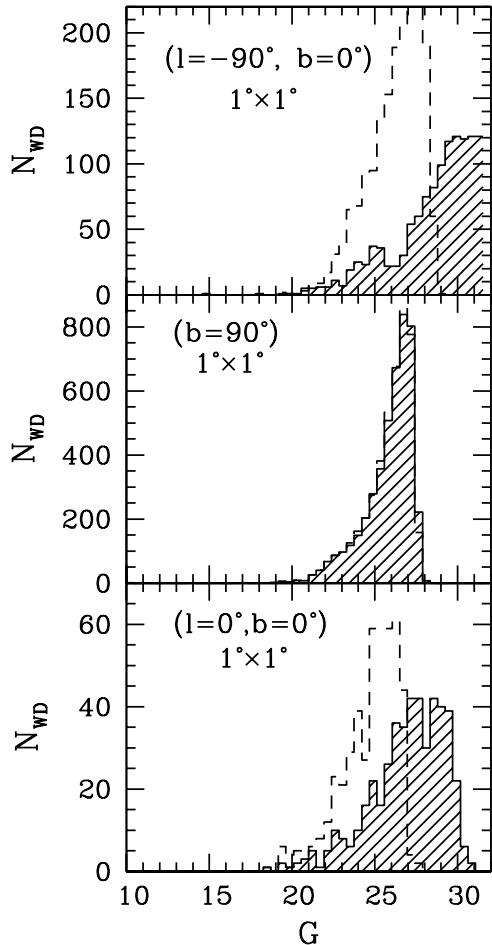


Figure 2. Total number of synthetic white dwarfs as a function of the *Gaia* apparent magnitude along the three small pencils beams discussed in the text. The shaded histograms correspond to the population obtained when Galactic extinction is taken into account, whereas the dashed lines correspond to the population obtained when Galactic extinction is neglected in the calculations.

Table 1. Number of disk white dwarfs for three patches of $1^\circ \times 1^\circ$ in different regions of the sky (see text for details).

	$G < 19$	$G < 20$	$G < 21$
$(l = -90^\circ, b = 0^\circ)$	6	9	13
$(l = 0^\circ, b = 0^\circ)$	5	11	13
$(l = 180^\circ, b = 0^\circ)$	6	11	15
$(b = 90^\circ)$	4	8	12
All sky	$2.1 \cdot 10^5$	$3.9 \cdot 10^5$	$5.2 \cdot 10^5$

with $M_v \simeq 16^{\text{mag}}$ — that of the observed cut-off of the disk white dwarf luminosity function — up to distances of 100 pc.

The total estimated number of white dwarfs within 100, 200, 300 and 400 pc can be found in the first row of table 2. Of these white dwarfs, those which pass the cut in G apparent magnitude for a limiting magnitude of 21 are given in the second row of table 2. The third row lists which of these will also have measurable proper motions. We have consid-

Table 2. Results of the Monte Carlo simulations of disk white dwarf population accessible to *Gaia*.

	100 pc	200 pc	300 pc	400 pc
$N_{\text{WD}}(9.0 < G < 29.0)$	11595	80775	273684	743893
$N_{\text{WD}}(G < 21)$	11593	57804	121474	226922
$N_{\text{WD}}(\mu > \mu_{\text{cut}})$	11593	57804	121472	226919
$\sigma_\mu/\mu < 0.10$	1.000	0.999	0.999	0.998
$\sigma_\mu/\mu < 0.01$	0.998	0.966	0.929	0.893
$\sigma_\pi/\pi < 0.10$	1.000	1.000	1.000	1.000
$\sigma_\pi/\pi < 0.01$	0.877	0.559	0.357	0.249
ν_{21}	0.999	0.716	0.444	0.305
$N_{\text{WD}}(G < 20)$	10391	34560	67067	123419
$N_{\text{WD}}(\mu > \mu_{\text{cut}})$	10391	34560	67067	123418
$\sigma_\mu/\mu < 0.10$	1.000	0.999	0.999	0.999
$\sigma_\mu/\mu < 0.01$	0.998	0.994	0.986	0.976
$\sigma_\pi/\pi < 0.10$	1.000	1.000	1.000	1.000
$\sigma_\pi/\pi < 0.01$	0.877	0.559	0.357	0.249
ν_{20}	0.896	0.428	0.245	0.166

ered that a white dwarf will have measurable proper motion when the error in proper motion is smaller than the proper motion itself. The completeness (ν_{21}) of the sample necessary to build the white dwarf luminosity function is assessed in the last row of this table. As can be seen, *Gaia* will be able to detect the whole white dwarf population within 100 pc, and roughly half of it within 300 pc, decreasing to one third at distances of 400 pc, which represents a huge step forward in our knowledge of the white dwarf population. The second and the third sections of table 2 assess the accuracy of the astrometric measurements. Most of the detected white dwarfs will have good determinations for both the parallax and the proper motion (σ_μ/μ and $\sigma_\pi/\pi < 0.1$) up to distances of more than 400 pc and superb accuracies (σ_μ/μ and $\sigma_\pi/\pi < 0.01$) will be obtained for half of the sample up to distances of about 200 pc. The last sections of table 2 list the same quantities for a limiting magnitude of 20. Obviously the overall performances and the completeness of the sample will be in this case smaller.

The same exercise can be done for the halo white dwarf population. However the results are not as encouraging as those obtained so far for the disk white dwarf population. The results for the halo white dwarf population are displayed in table 3 and figure 4. Perhaps the most important result of this set of simulations is that the number of halo white dwarfs which *Gaia* will be able to observe is likely to be of the order of a few hundreds, thus increasing enormously the total number of halo white dwarf candidates, which presently is of order 10 or less. However, the completeness of the sample even for 100 pc will be small — $\sim 50\%$ for a limiting magnitude of 21 and only $\sim 20\%$ for a limiting magnitude of 20 — and decreasing rapidly for larger distances. Most importantly, *Gaia* will only be able to observe the bright portion of the halo white dwarf luminosity function. Hence, a direct determination of the age of the halo using the cut-off of the halo white dwarf luminosity function will not be pos-

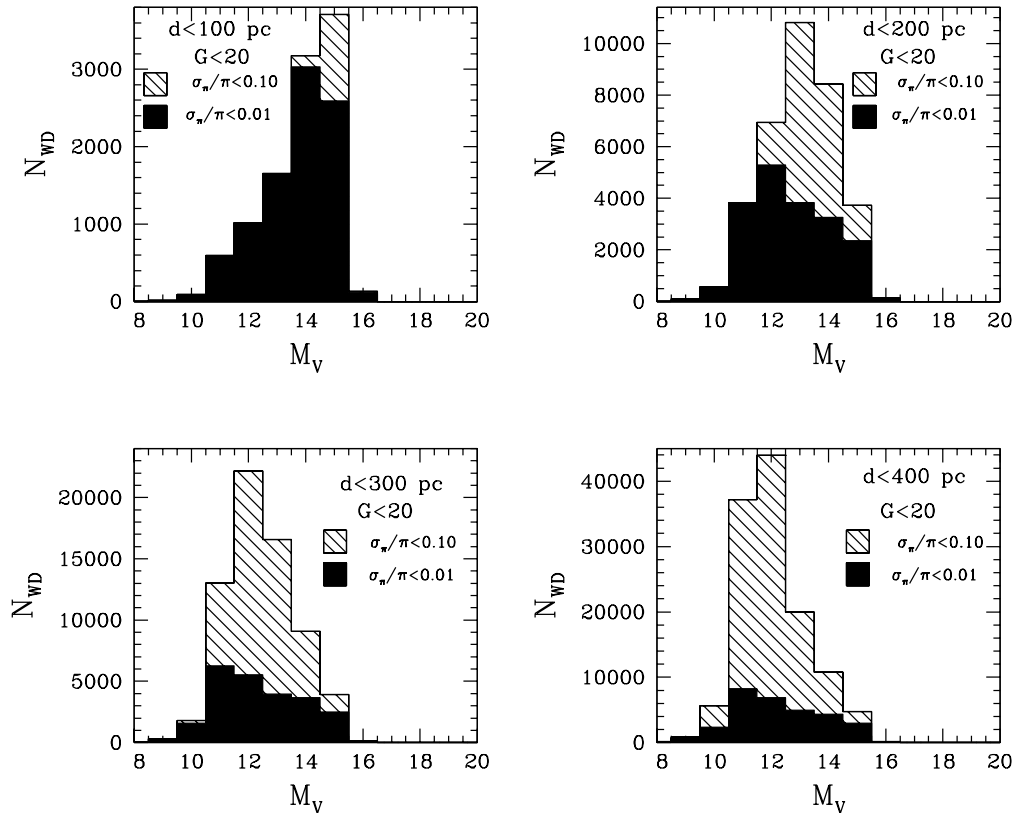


Figure 3. Distribution of the number of disk white dwarfs detected by *Gaia* as a function of their absolute magnitude according to their errors in parallax, for different distances.

Table 3. Same as table 2 for the halo white dwarf population.

	100 pc	200 pc	300 pc	400 pc
$N_{\text{WD}}(9.0 < G < 29.0)$	359	2737	9174	21505
$N_{\text{WD}}(G < 21)$	192	434	726	1099
$N_{\text{WD}}(\mu > \mu_{\text{cut}})$	192	434	726	1099
$\sigma_{\mu}/\mu < 0.10$	1.000	1.000	1.000	1.000
$\sigma_{\mu}/\mu < 0.01$	1.000	1.000	0.998	0.995
$\sigma_{\pi}/\pi < 0.10$	1.000	1.000	1.000	1.000
$\sigma_{\pi}/\pi < 0.01$	0.905	0.636	0.395	0.260
ν_{21}	0.535	0.158	0.079	0.051
$N_{\text{WD}}(G < 20)$	84	195	344	542
$N_{\text{WD}}(\mu > \mu_{\text{cut}})$	84	195	344	542
$\sigma_{\mu}/\mu < 0.10$	1.000	1.000	1.000	1.000
$\sigma_{\mu}/\mu < 0.01$	1.000	1.000	0.998	1.000
$\sigma_{\pi}/\pi < 0.10$	1.000	1.000	1.000	1.000
$\sigma_{\pi}/\pi < 0.01$	0.905	0.636	0.395	0.260
ν_{20}	0.234	0.071	0.038	0.025

sible. Despite all this, the accuracy of the measurements of those halo white dwarfs detected by *Gaia* will be impressive since we will have extremely precise parallaxes for a good fraction of halo white dwarfs with distances of up to 400 pc, independently of the limiting magnitude.

3.2 Classifying halo and disk white dwarfs

The natural question which arises now is how to distinguish halo white dwarfs from disk white dwarfs. Obviously, due to gravitational settling in the atmospheres of white dwarfs the metallicity cannot be used. Although *Gaia* will be able to obtain radial velocities using the SPECTRO instrument it is unlikely that *Gaia* could determine the full three-dimensional velocities of white dwarfs, since the SPECTRO instrument will be optimized for $G < 17$ main sequence stars. The reduced proper motion diagram can be of great help in distinguishing disk and halo members. An example of the expected reduced proper motion diagram that *Gaia* will obtain is shown in figure 5. As can be seen there, the reduced proper motion $H = M_V - 5 \log \pi + 5 \log \mu$ is a good indicator of the membership to a given population. Simulated halo white dwarfs occupy a clear locus in this diagram. However, for $V - I \lesssim 0.2$ the identification becomes less clear. Also shown in figure 5 is the line $H_0 = 7(V - I) + 17.2$. Clearly, white dwarfs with $H > H_0$ can be preliminarily ascribed to the halo white dwarf population. In order to make quantitative statements we introduce the confusion matrix:

$$C_H = \begin{pmatrix} 0.68 & 0.05 \\ 0.32 & 0.95 \end{pmatrix} \quad (12)$$

where the matrix element C_H^{11} indicates the percentage of disk white dwarfs classified as “disk”, C_H^{21} is the percentage of disk stars misclassified as “halo”, and so on. Hence, the reduced proper motion, H , turns out to be a reasonable membership discriminator.

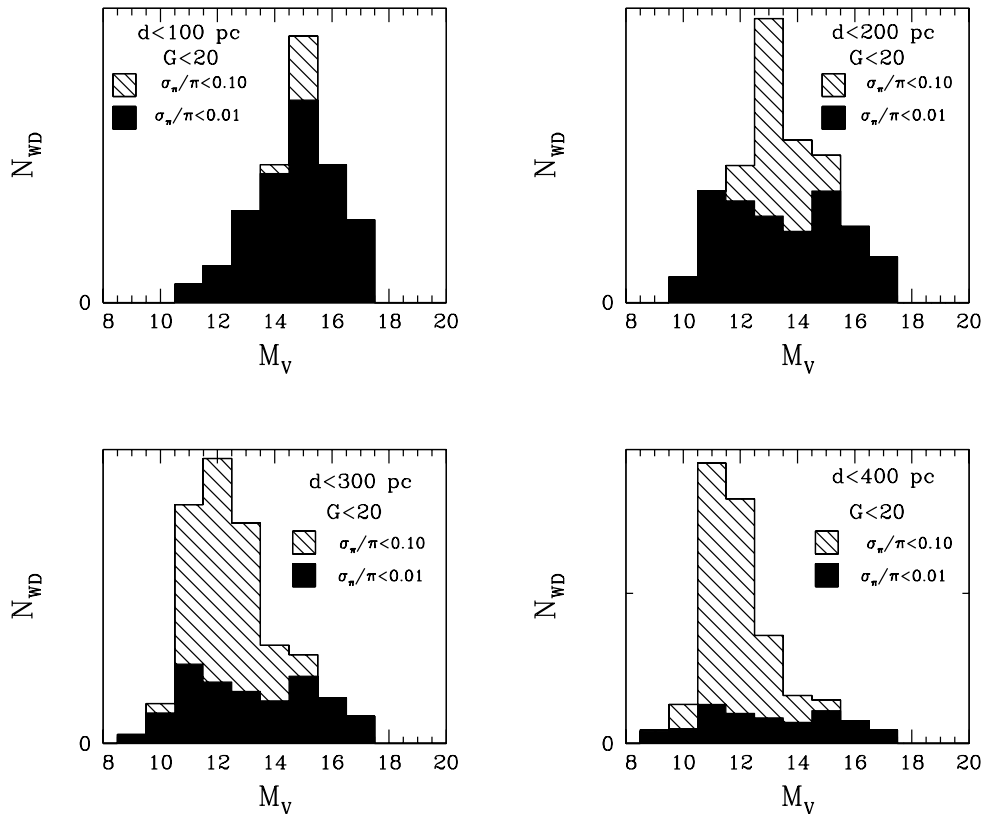


Figure 4. Same as figure 3 for the halo white dwarf population.

In order to provide a more consistent and easy method to ascertain the population membership of white dwarfs we proceed in the spirit of Salim & Gould (2003). That is, we introduce a discriminator η , by which we classify stars as a function of their position in the reduced proper motion diagram, their colour, and their Galactic latitude:

$$\eta = H + C_1(V - I) + C_2|\sin b| + C_3 \quad (13)$$

where the constants C_1 , C_2 and C_3 are computed in such a way that the distance, s , between the halo and the disk white dwarf populations is maximum:

$$s = \sum_i^{N_D} \sum_j^{N_H} (\eta_i - \eta_j)^2 \quad (14)$$

where N_D and N_H are, respectively, the number of simulated disk and halo white dwarfs.

The value of the constants obtained in such a way are $C_1 = 0.48$, $C_2 = 0.40$ and $C_3 = -4.83$. This membership discriminator works slightly better than the reduced proper motion and distinguishes between disk and halo white dwarfs, but, again, only for those white dwarfs with colour indices $V - I \gtrsim 0.2$. Moreover, those white dwarfs with $\eta > \eta_0 = 3(V - I) + 13.1$ can be considered as good bona-fide halo white dwarfs. It is interesting to realize that less disk white dwarfs are misclassified as halo members and vice versa. In fact the confusion matrix is in this case:

$$C_\eta = \begin{pmatrix} 0.73 & 0.06 \\ 0.27 & 0.94 \end{pmatrix} \quad (15)$$

Figure 6 demonstrates the difficulty of recovering halo white dwarfs. In this figure we show the distribution of our

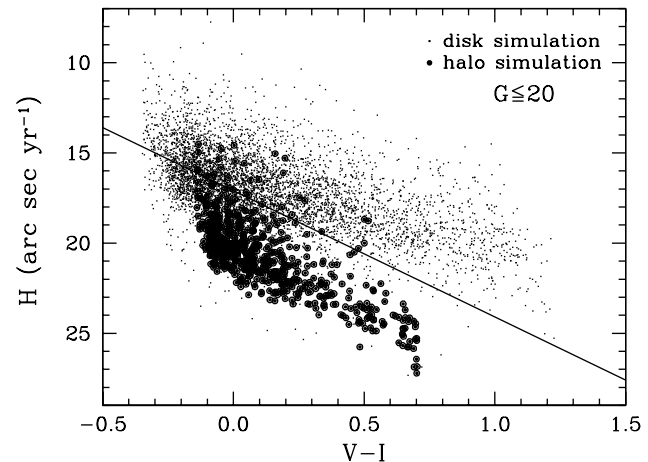


Figure 5. Reduced proper motion diagram for the disk — small solid dots — and halo — large open circles — simulations. Only those white dwarfs with $m_G < 20$ have been considered. For the sake of clarity only 5% of the simulated disk white dwarfs have been plotted.

membership discriminator for both the halo and disk white dwarf populations. Both distributions are shown in a logarithmic scale for the sake of clarity. By examining this figure it turns out that the distribution of halo white dwarfs cannot be clearly discriminated from that of the disk. Moreover, disk white dwarfs outnumber halo members. Both distributions are approximately gaussian, and the average values and standard deviations of the membership discriminator

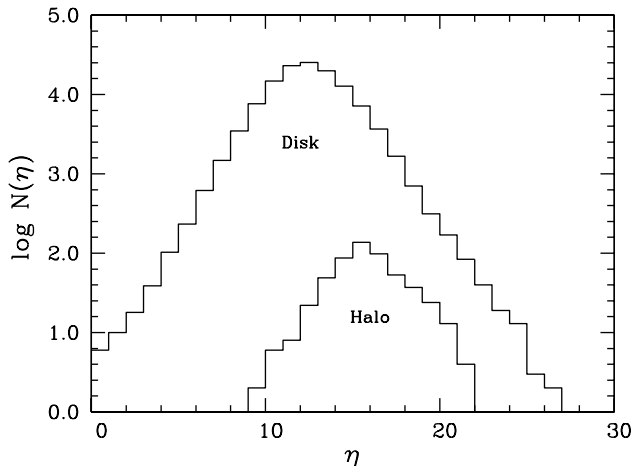


Figure 6. Distribution of the membership discriminator η . A logarithmic scale has been used for the sake of clarity.

for the disk and halo white dwarf populations turn out to be $\langle \eta_D \rangle \simeq 12.4 \pm 2.3$ and $\langle \eta_H \rangle \simeq 16.1 \pm 2.2$, respectively. Using this membership discriminator 82% and 83% of the whole disk and halo white dwarf populations are correctly classified at the 1σ level. It must be noted, however, that an artificial intelligence algorithm (Torres et al. 1998; García-Berro et al. 2003a) can be successfully used to classify white dwarfs, and that the results obtained using that algorithm are considerably better, since only 2% of disk white dwarfs are erroneously classified as halo white dwarfs using advanced classification techniques.

3.3 The disk white dwarf luminosity function

Now that we have assessed the total number counts of disk white dwarfs we pay attention to some specific matters regarding the disk white dwarf luminosity function. In particular we ask to what precision the age of the Galactic disk can be estimated. In Fig. 7 we show the average of 40 independent realizations of the disk white dwarf luminosity function for several disk ages. Each curve is labelled with its corresponding age. The error bars are the standard deviation of the 40 independent realizations. The white dwarf luminosity functions have been computed using the $1/V_{\max}$ method (Schmidt 1968). Hence, a set of restrictions is needed for selecting a subset of white dwarfs which, in principle, should be representative of the whole white dwarf population. We have chosen the following criteria for selecting the final sample: $G \leq 20^{\text{mag}}$ and no restriction in proper motion. The reason for this choice is quite simple. From the discussion in §3.1 it is clear that the sample of disk white dwarfs that *Gaia* will eventually detect is almost complete in magnitude up to $G \simeq 20$, and all white dwarfs within this sample will have measurable proper motions. Consequently, the proper motion cut does not play any role at all. This is in sharp contrast with the adopted magnitude and proper motion cuts actually in use to derive the observed disk white dwarf luminosity function: $m_V \leq 18.5^{\text{mag}}$ and $\mu \geq 0.16'' \text{ yr}^{-1}$ (Oswalt et al. 1996). Additionally, and since the number of white dwarfs that are used in building the disk white dwarf luminosity function is much larger than the size of the actual

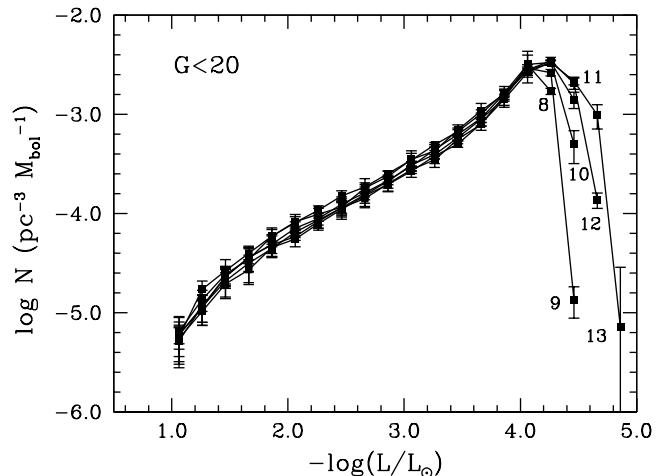


Figure 7. Luminosity function of disk white dwarfs for several ages of the disk, ranging from 8 to 13 Gyr, with an interval of 1 Gyr. The error bars are the standard deviation of the 40 independent realizations. See text for details.

Table 4. Expected statistical errors in the determination of the age of the disk, as obtained from fitting the cut-off in the disk white dwarf luminosity function, in terms of the age of the disk. See text for details.

T_{disk} (Gyr)	ΔT_{disk} (Gyr)
8	0.15
9	0.30
10	0.30
11	0.30
12	0.15
13	1.13

sample of white dwarfs with known parallaxes and proper motions we have binned the luminosity function in smaller luminosity bins. To be precise, the binning is five bins per decade.

Fig. 7 clearly shows that the error bars are small enough to secure a reliable determination of the age of the disk, using the observed cut-off in the disk white dwarf luminosity function. The easiest and more straightforward way to assess the statistical errors associated with the measurement of the age of the disk is trying to reproduce the standard procedure. That is, we have fitted the position of the “observational” cut-off of each of the Monte Carlo realizations with a standard method (Hernanz et al. 1994) to compute the white dwarf luminosity function using *exactly* the same inputs adopted to simulate the Monte Carlo realizations, except, of course, the age of the disk, which is the only free parameter. To be more precise, we compute the disk white dwarf luminosity function according to:

$$n(L) \propto \int_{M_i}^{M_s} \Psi(T_{\text{disk}} - t_{\text{cool}}(L, M_{\text{MS}}) - t_{\text{MS}}(M_{\text{MS}})) \Phi(M_{\text{MS}}) \tau_{\text{cool}}(L, M_{\text{MS}}) dM_{\text{MS}} \quad (16)$$

where $\Phi(M_{\text{MS}})$ is the initial mass function, $\Psi(t)$ the star formation rate, $t_{\text{cool}}(L, M_{\text{MS}})$ the cooling time, $t_{\text{MS}}(M_{\text{MS}})$ the

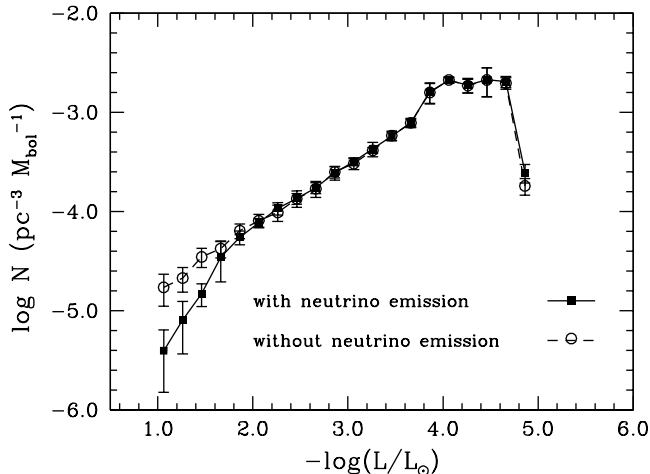


Figure 8. Luminosity function of disk white dwarfs for two different sets of cooling curves. The solid squares connected by a solid line correspond to the case in which neutrino emission was properly taken into account, whereas the open circles connected by a dashed line correspond to the case in which neutrino emission was neglected. See text for details.

main sequence lifetime and $\tau_{\text{cool}}(L, M_{\text{MS}})$ the characteristic cooling time. Moreover, for each independent realization we have fitted the “theoretical” white dwarf luminosity functions not only to the average value of the disk white dwarf luminosity function as obtained from our Monte Carlo simulations but also to the corresponding upper and lower values allowed by the error bars. In this way we end up with an estimate of the error in determining the disk age. The results are shown in table 4. As can be seen the errors will be small. The typical error estimate obtained using the actually observed white dwarf luminosity function is 1.5 Gyr, 5 times larger. Hence, *Gaia* will allow a precise determination of the age of the Galactic disk which may be compared with that obtained using other methods, like turn-off stars and isochrone fitting. In this case, moreover, it should be taken as well into account that *Gaia* will allow very rigorous tests of the main sequence and red giant stellar evolutionary models, so additional information will be available to constrain the (pre-white dwarf) stellar models.

Next we ask ourselves if *Gaia* will be able to discriminate between different cooling curves and, hence, to place constraints on the physical mechanisms operating during the cooling process. More specifically, we want to show here that *Gaia* will be able to place constraints both on the mechanisms operating at high effective temperatures — basically neutrino cooling — and on the mechanisms which are dominant for relatively low core temperatures (crystallization).

Neutrinos are the dominant form of energy loss in model white dwarf stars down to $\log(L/L_{\odot}) \simeq -2.0$, depending on the stellar mass. As a consequence, the evolutionary timescales of white dwarfs at these luminosities sensitively depend on the ratio of the neutrino energy loss to the photon energy loss, and, hence, the slope of the white dwarf luminosity function directly reflects the importance of neutrino emission. Although the unified electroweak theory of lepton interactions that is crucial for understanding neutrino production has been well tested in the high-energy regime

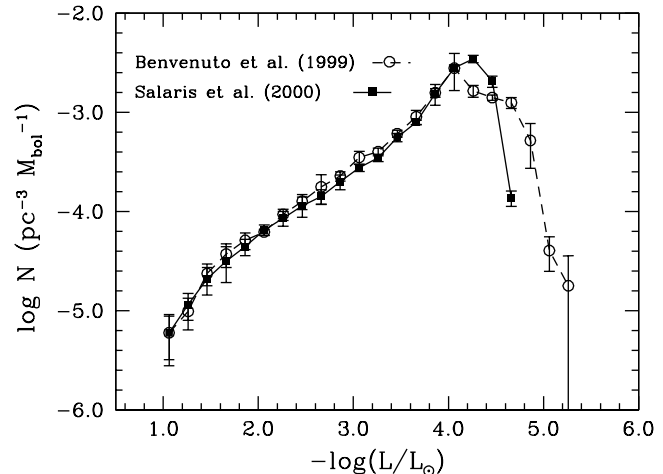


Figure 9. Luminosity function of disk white dwarfs for two different sets of cooling sequences. The solid squares connected by a solid line correspond to the white dwarf luminosity function obtained when the cooling sequences of Salaris et al. (2000) are used, whereas the open circles connected by a dashed line correspond to the white dwarf luminosity function obtained when the set of cooling sequences of Benvenuto & Althaus (1999) are used.

— see, for instance, Hollik (1997) for an excellent review — the approach presented here should result in an interesting low-energy test of the theory. To this regard in Fig. 8 we show two disk white dwarf luminosity functions for which we have adopted different prescriptions for the cooling curves. In both cases we have adopted the evolutionary cooling sequences of Benvenuto & Althaus (1999). However in one of the sequences (corresponding to open circles connected by a dashed line) neutrino emission has been artificially inhibited. In passing we also note that, opposite to what has been done so far, and for the sake of simplicity in this set of simulations we have adopted a *single* cooling sequence, corresponding to that of an average-mass $0.6 M_{\odot}$ white dwarf made of pure oxygen. Fig. 8 clearly shows that the drop-off in the white dwarf luminosity function is not affected by the inclusion of the neutrino emissivity, as should be expected given that the neutrino-dominated cooling phase is very short in all cases. However the slope of the disk white dwarf luminosity function, which reflects the cooling rate, is sensitive to the treatment of neutrinos. More interestingly, *Gaia* will be able to measure the cooling rate and, thus, to probe the electroweak theory at low energies.

After examining the physical mechanisms that operate at moderately high luminosities, say $\log(L/L_{\odot}) \gtrsim -2.0$, we focus now on one of the crucial issues in the theory of white dwarf cooling, namely on crystallization and phase separation at low core temperatures ($T_c \sim 10^6$ K). In order to make reliable comparisons we adopt besides our own cooling sequences (Salaris et al. 2000) those of Benvenuto & Althaus (1999). This set of cooling sequences is available for all the masses of interest, uses a modern equation of state and the internal chemical profiles of Salaris et al. (1997). The only major difference between both sets of cooling sequences is the treatment of phase separation upon crystallization which in the case of the cooling sequences of Salaris et al. (2000) was properly taken into account, whereas in the cooling sequences of Benvenuto & Althaus (1999) it was

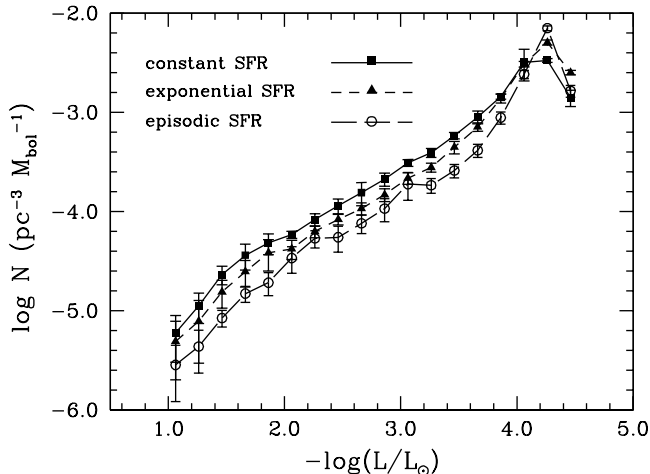


Figure 10. Luminosity function of massive disk white dwarfs for several star formation histories. The solid line corresponds to a constant volumetric star formation rate. The long dashed line corresponds to an episodic star formation rate and the short dashed solid line corresponds an exponentially decreasing star formation rate.

disregarded. As discussed in Isern et al. (1997) the inclusion of phase separation upon crystallization adds an extra delay to the cooling (and, thus, considerably modifies the characteristic cooling times at low luminosities), which depends on the initial chemical profile (the ratio of carbon to oxygen) and on the transparency of the insulating envelope. In both sets of cooling sequences the thicknesses of the helium buffer and of the overlying hydrogen envelope are the same. Thus, the disk white dwarf luminosity function computed with those sets of cooling sequences should mostly reflect the treatment of crystallization. This is illustrated in Fig. 9, where the luminosity functions computed with the cooling sequences of Salaris et al. (2000) — solid squares connected with a solid line — and with the cooling sequences of Benvenuto & Althaus (1999) for a disk age of 12 Gyr are displayed. Note that for moderately high luminosities — namely $\log(L/L_\odot) \gtrsim -4.0$ — the agreement between both sets of calculations is very good. Obviously, for the same disk age, the cut-off of disk white dwarf luminosity function computed with the cooling sequences of Benvenuto & Althaus (1999) moves to lower luminosities, $\log(L/L_\odot) \simeq -5.0$. Consequently, if a direct measure of the disk age with reasonable precision is obtained by an independent method, say via turn-off stars, *Gaia* will directly probe the physics of crystallization. It is worth noting as well that not only the exact location of the drop-off of the disk white dwarf luminosity function is affected by the details of the cooling sequences but also, the position and the shape of the maximum of the white dwarf luminosity function, thus allowing additional tests.

Now we turn our attention to how the disk white dwarf luminosity function may be used to derive the Galactic star history. We have computed a series of models in which we have adopted different star formation rates. In all cases the adopted age of the disk was 12 Gyr. For the first of our models we have adopted (as earlier in the paper) a constant volumetric star formation rate. The second star formation rate is on which is exponentially decreasing with an e-folding

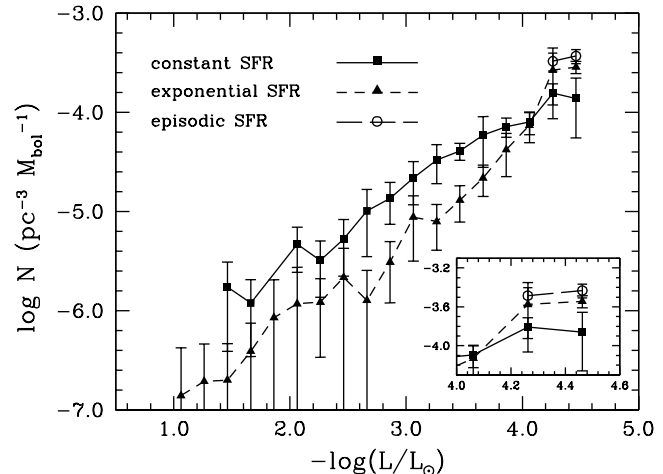


Figure 11. Luminosity function of massive disk white dwarfs for several star formation histories. The solid line corresponds to a constant volumetric star formation rate. The long dashed line corresponds to an episodic star formation rate and the short dashed solid line corresponds an exponentially decreasing star formation rate. The inset shows an expanded view of the region near the maximum of the luminosity function, where the episodic star formation rate can be better observed.

time $\tau = 4$ Gyr. Finally, our last adopted star formation rate corresponds to episodic star formation, for which we have adopted a burst of constant strength that started 1 Gyr after the formation of the disk and lasting for 3 Gyr. For the rest of the time the star formation activity considered in this case was zero. The results are shown in Fig. 10. As can be seen the white dwarf luminosity will be sensitive to the star formation history. However, recovering the exact dependence of the star formation history will be difficult since the inverse problem must be solved (Isern et al. 1995). From Eq. (16) it is clear that the origin of the problem is the long lifetimes of low mass main sequence stars (Isern et al. 1995; García-Berro et al. 2003b). This implies that the past star formation activity is still influencing the present white dwarf birthrate. This can be clearly seen in Fig. 10. In order to solve Eq. (16) for the star formation rate there exist two alternatives. The first and most straightforward method requires an “a priori” knowledge of the shape of the star formation history and consists in adopting a trial function, depending on several parameters, and search for the values of these parameters that best fit the observed luminosity function by minimizing the differences between the observational and the computed luminosity function (Isern et al. 2001). The second possibility consists in computing the luminosity function of massive white dwarfs (Díaz-Pinto et al. 1994; Isern et al. 1999), which have negligible main sequence lifetimes, thus making much easier the solution of the inverse problem.

In our simulations we obtain a sizeable fraction of massive white dwarfs, those with masses larger than say $0.8 M_\odot$, which varies from 7% for the constant star formation history, to 4% for the exponential one and to 3% for the episodic star formation history. These fractions are enough to obtain the history of the star formation activity in the solar neighborhood (Díaz-Pinto et al. 1994). Although these fractions may seem small when taken at face value, the absolute numbers

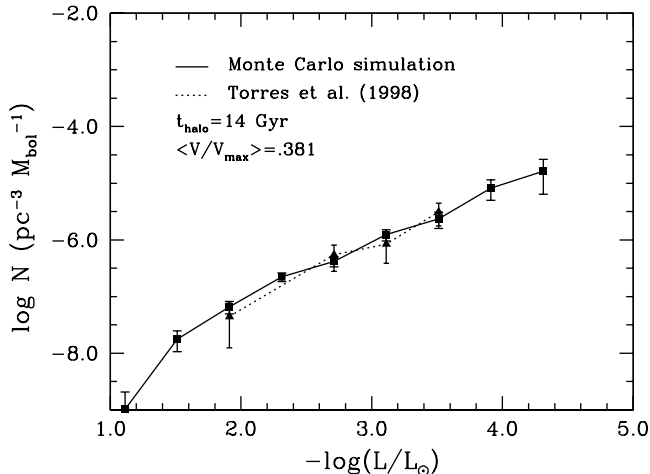


Figure 12. Luminosity function of halo white dwarfs. The solid line corresponds to the simulations presented here, assuming a recovery fraction of 50%. The dashed line is the luminosity function of Torres et al. (1998). See text for further details.

of massive white dwarfs are impressive, since for the case of a constant star formation rate, 700 massive white are expected to be found, whereas for the other two star formation histories 500 and 300 massive white dwarfs will be found respectively, thus allowing a determination of the luminosity function of massive white dwarfs. Such luminosity functions are shown in Fig. 11 for the three star formation rates studied here. As this figure clearly shows we will be able to obtain a reliable determination of the star formation rate. It is interesting to note that the slopes of the luminosity functions computed with a constant and an exponentially decreasing star formation rates are quite different now, in contrast with the behavior shown in Fig. 10. Moreover the contribution of the episodic star formation rate is concentrated in the very last luminosity bins.

3.4 The halo white dwarf luminosity function

In figure 12 we show the luminosity function of halo white dwarfs that *Gaia* will observe for a halo age of 14 Gyr, and assuming that only 50% of the halo white dwarfs with $H < 18$ and $V - I < 0.3$ are correctly classified as halo white dwarfs. As borne out from Fig. 12, *Gaia* will be able to measure only the bright portion of the white dwarf luminosity function of halo white dwarfs, which carries valuable information about the initial mass function. However, the cut-off of the luminosity function — which provides an independent estimate of the age of the stellar halo — will not be detected. This is obviously due to the cut in magnitudes of *Gaia*, which will be $G \sim 20^{\text{mag}}$. According to this magnitude cut and given that the age of the stellar halo is $t_{\text{halo}} \gtrsim 13$ Gyr, a considerable fraction of halo white dwarfs will not be detected by *Gaia*. This is assessed in Fig. 13, where the distribution of white dwarfs with $G < 20$ — those detectable by *Gaia* — is compared to the total population of halo white dwarfs. Clearly, very few halo white dwarfs with magnitudes close to that of the cut-off will be observed by *Gaia*, thus preventing us to directly measure the age of the Galactic halo.

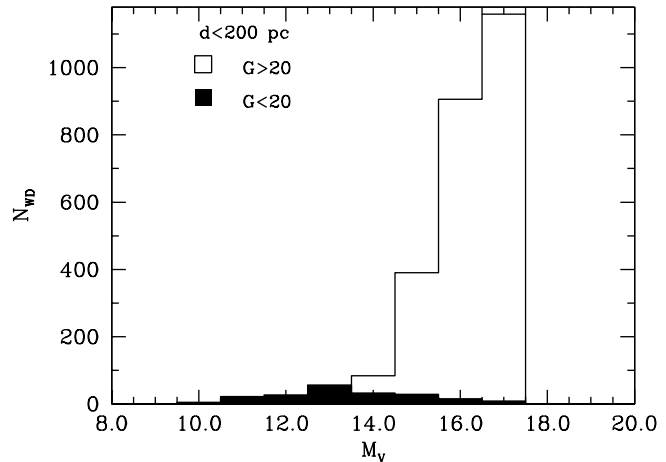


Figure 13. Distribution of halo white dwarfs detected by *Gaia* (solid histogram) compared to the distribution of the simulated sample of halo white dwarfs (empty histogram), for an halo age of 14 Gyr, and a recovery fraction of 50%.

One important concern is whether or not the advanced classification techniques mentioned above are mandatory in order to obtain a reliable luminosity function. In order to check this issue we have proceeded as follows. First we have assumed that we are able to distinguish between halo and disk candidates with a success rate of 100%. After this, in a second set of calculations we have assumed that only 50% of halo white dwarfs are correctly recovered in the region delimited by $H < 18$ and $V - I < 0.3$. Finally, in a third set of calculations we have adopted a recovery fraction of 25% within this region. The halo white dwarf luminosity function presented in figure 12 corresponds to the second case. However, we have found that the results are relatively insensitive to the recovery fraction. The reason for this behaviour is easy to understand: the region in which disk and halo white dwarfs are not well identified corresponds precisely to the brightest white dwarfs and, hence, to luminosities for which the density of white dwarfs per unit bolometric magnitude is very small. Consequently, although *Gaia* will only determine the bright portion of the halo white dwarf luminosity function, there will not be serious systematic errors for luminosities $\log(L/L_{\odot}) \gtrsim -2.0$.

As we have shown, it is not expected that *Gaia* will directly measure the age of the Galactic halo by finding white dwarfs at the end of the halo white dwarf cooling sequence. However, one could imagine that the halo age could be still be somehow constrained since a younger halo could generate stars above the *Gaia* magnitude limit. In Fig. 14 we explore such possibility by adopting several halo ages and, again, assuming a recovery fraction of 50%. This figure clearly shows that for reasonable halo ages this is not the case, since the drop-off of the white dwarf luminosity function is located at luminosities well beyond the capabilities of *Gaia*, as anticipated in Isern et al. (1998a).

In Fig. 15 we explore the sensitivity of the halo white dwarf luminosity function to the choice of the initial mass function. As we have done so far we have adopted a halo age of 12 Gyr and an age spread of 1 Gyr. We have simulated two halo white dwarf populations, the first one according to

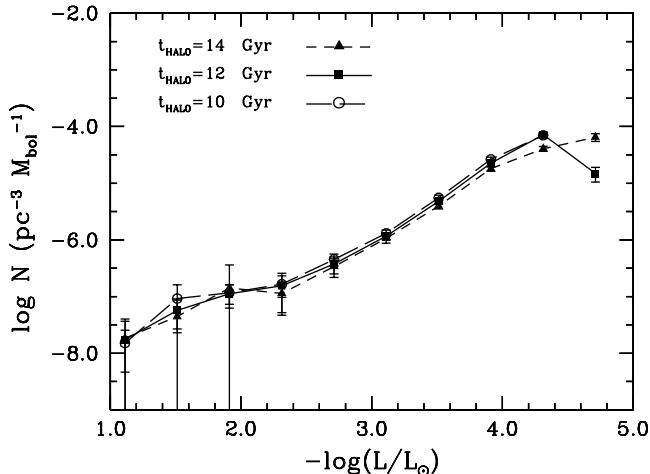


Figure 14. White dwarf luminosity functions for several halo ages, ranging from 10 to 14 Gyr, assuming a recovery fraction of 50%.

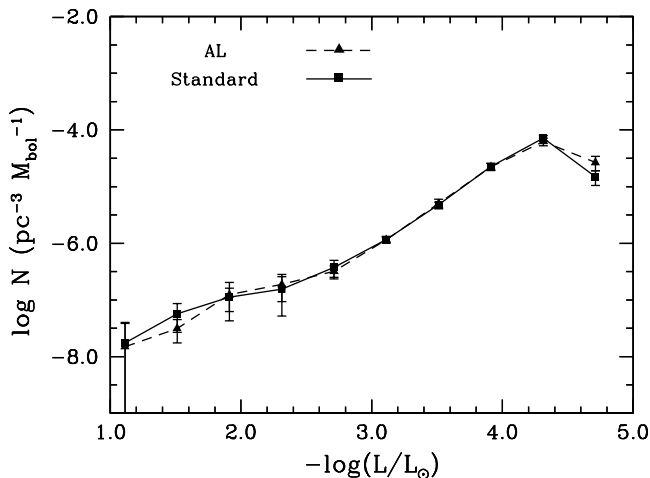


Figure 15. Halo white dwarf luminosity functions for two initial mass functions, adopting a halo age of 12 Gyr and an age spread of 1 Gyr, again assuming a recovery fraction of 50%.

the initial mass function of Adams & Laughlin (1996) and the second one to our standard initial mass function (Scalo 1998). Unfortunately *Gaia* will not be able to distinguish between these initial mass functions, as figure 15 clearly shows.

This is not surprising at all. Assuming that the halo was formed in a burst of star formation of negligible duration, then for all white dwarfs we have:

$$t_{\text{HALO}} \simeq t_{\text{MS}}(M_{\text{MS}}) + t_{\text{cool}}(L, M_{\text{MS}}) \quad (17)$$

This means that, given an age of the halo, t_{HALO} , there exists a function $M_{\text{MS}} = M_{\text{MS}}(L)$ or, in other words, that the white dwarfs contributing to each luminosity bin of the white dwarf luminosity function have the same mass. Taking this into account we have:

$$n(L) \simeq \frac{dn}{dM_{\text{MS}}} \frac{dM_{\text{MS}}}{dL} = \Phi(M_{\text{MS}}) \frac{dM_{\text{MS}}}{dL} \quad (18)$$

The first term in this equation is the initial mass function, whereas the second term is related to the cooling times. Hence, provided that we have reliable characteristic cooling

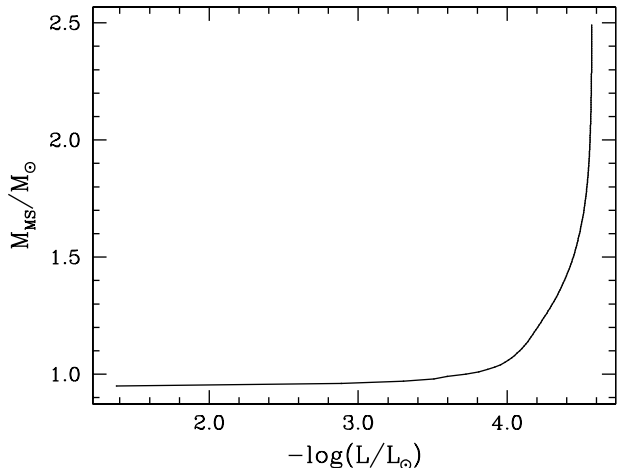


Figure 16. Mass in the main sequence contributing to each luminosity bin for a burst of star formation of negligible duration which happened 12 Gyr ago.

times, the halo white dwarf luminosity function could be eventually used to retrieve useful information about the initial mass function of the halo, if different from that of the disk populations. However, most of the information regarding the initial mass function concentrates in the low luminosity bins. In particular, in Fig. 16 we show the the mass of the main sequence which contributes to each luminosity bin of the halo white dwarf luminosity function. As can be seen there $M_{\text{MS}}(L)$ remains almost flat up to luminosities of the order of $\log(L/L_{\odot}) \simeq -3.5$, and then a very steep rise can be observed. As we have already discussed, the number of halo white dwarfs of these very low luminosities that *Gaia* will probably observe is small and, consequently, will not allow us to draw definite conclusions about the shape of the initial mass function.

Finally, in Fig. 17 we explore the effects in the luminosity function of halo white dwarfs of different age spreads of the adopted burst of star formation. We have adopted a halo age of 12 Gyr, whereas the durations of the star formation bursts were 2 Gyr (short dashed line and solid triangles), 1 Gyr (solid line and filled squares) and 0.5 Gyr (long dashed line and open circles). As shown in Fig. 17 the three curves are almost indistinguishable, thus preventing us from obtaining a better understanding the process of formation of the Galactic halo by using the luminosity function of halo white dwarfs. The reason is quite simple and related to the behavior of $M_{\text{MS}}(L)$ as shown in Fig. 16. In particular, we have that for the duration of the bursts of star formation adopted here (2, 1 and 0.5 Gyr) — which we believe cover a realistic range of age spreads — the corresponding masses of the white dwarfs just entering into the cooling phase are, respectively, 0.57, 0.59 and 0.61 M_{\odot} , and thus their respective characteristic cooling times, τ_{cool} , are very similar. Since at luminosities of $\log(L/L_{\odot}) \approx -2$ the function $M_{\text{MS}}(L)$ is almost flat, the bright branch of the luminosity function only reflects the speed of cooling, washing out any other information (Isern et al. 1998a).

4 CONCLUSIONS AND DISCUSSION

In this paper we have explored the impact *Gaia* will have on our understanding of the Galactic white dwarf population. We have shown that the superb astrometric capabilities of *Gaia* will provide us with an unprecedented number of white dwarfs with excellent astrometric measurements. In particular we have shown that the disk white dwarf population will be probed up to distances of 400 pc, with typical errors smaller than 10%, both in proper motion and parallax and with a completeness ranging from nearly 100% for objects within 100 pc to 30% for objects within 400 pc, when a magnitude cut of $G_{\text{cut}} = 21$ is adopted. The performances, of course, are worse for a magnitude cut of 21. Thus, *Gaia* will determine with high accuracy the disk white dwarf luminosity function and its drop-off. We have also shown that this excellent situation will not pertain for the halo white dwarf population. In particular, although the astrometric measurements will be highly accurate as well, the completeness of the survey will be much smaller, typically 50% within 100 pc. We have also analyzed how to distinguish between halo and disk white dwarfs and we have demonstrated that although the reduced proper motion diagram will be of some help in this regard, advanced classification techniques will be required to extract the maximum amount of information from the halo white dwarf population. Finally, we have also studied what would be the typical disk and halo white dwarf luminosity functions that *Gaia* will eventually obtain, and we have analyzed what could be the attainable scientific goals. We have found that the disk white dwarf luminosity function will constrain the age of the Galactic disk with good accuracy, using the observed drop-off in the disk white dwarf luminosity function, very much improving the present day constraints. *Gaia* will provide very precise information on the physical mechanisms (crystallization, phase separation, etc) operating during the cooling process by comparing the theoretical luminosity functions of disk white dwarfs with the observations. The luminosity function of massive disk white dwarfs will constrain the star formation history of the Galactic disk, whereas the lower mass white dwarfs will offer few constraints. For the halo we have found that only the bright portion will be accessible to *Gaia*, thus preventing us from getting valuable information about the initial mass function of the Galactic halo, or even its age or the duration of hypothetical burst of star formation which led to its formation (at least from its white dwarfs).

White dwarfs are well studied objects and the physical processes that control their evolution are reasonably well understood — see, for instance, the reviews of Isern et al. (1998b), Koester (2002), Hansen & Liebert (2003) and Isern & García-Berro (2004) — at least up to moderately low luminosities — of the order of $\log(L/L_{\odot}) = -3.5$. In fact, most phases of white dwarf evolution can be successfully characterized as a cooling process. That is, white dwarfs slowly radiate at the expense of the residual gravothermal energy. The release of this energy lasts for long time scales (of the order of the age of the Galactic disk $\sim 10^{10}$ yr). The mechanical structure of white dwarfs is supported by the pressure of the gas of degenerate electrons, whereas the partially degenerate outer layers control the flow of energy. Precise spectrophotometric data — like those that *Gaia* will provide — would certainly introduce very tight constraints

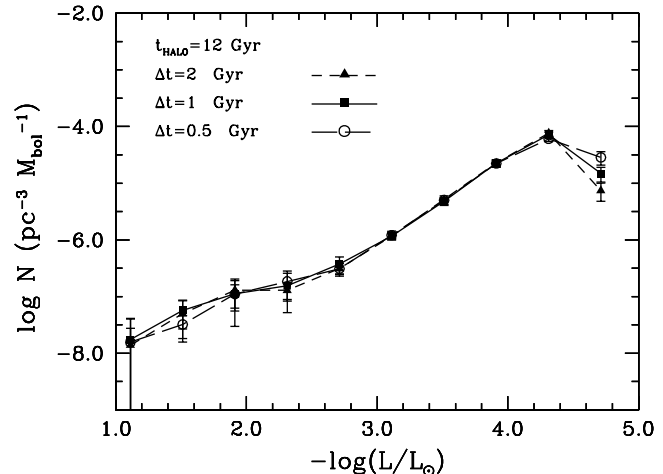


Figure 17. White dwarf luminosity functions for several age spreads of the Galactic halo ranging from 0.5 to 2.0 Gyr, again assuming a recovery fraction of 50%.

on the models. Specifically, *Gaia* will allow us to test the mass–radius relationship, which is still today not particularly well tested, by analyzing the spectrophotometric data of white dwarfs with known parallaxes — which will be of the order of several hundreds (see table 3). By comparing the theoretical models with the observed properties of white dwarfs belonging to binary systems, *Gaia* will also be able to constrain the relation between the mass in the main sequence and the mass of the resulting white dwarf.

Given their long cooling timescales, white dwarfs have been used as a tool to extract useful information about the past history of our Galaxy. The large number of white dwarfs that *Gaia* will observe will allow us to probe the structure and dynamics of the Galaxy as a whole, tracing back a hypothetical merger episode in the Galactic disk (Torres et al. 2001). Moreover, it will provide new clues about the halo white dwarf population and its contribution to the mass budget of our Galaxy — see, for instance, Isern et al. (1998a), Torres et al. (2002) and García-Berro et al. (2004), and references therein. Additionally, the disk white dwarf luminosity function has been used to derive constraints on the rate of variation of the gravitational constant (García-Berro et al. 1995). The accuracy of this bound is mainly limited by the statistical significance of the very last bins of the white dwarf luminosity function. Given the huge step forward that *Gaia* will introduce in the number counts of disk white dwarfs it is foreseeable that a very tight upper limit on \dot{G}/G will become eventually available. This, in turn, will pose tight constraints in current theories with extra dimensions (Lorén-Aguilar et al. 2003).

In summary, in this work we have shown how an astrometric mission like *Gaia* could dramatically increase the number of white dwarfs accessible to good quality observations. The increase of the observational database will undoubtedly have a large impact in our current understanding of the history and structure of the Galaxy as well as on the theoretical models of white dwarf cooling, which, in turn, will certainly influence our knowledge of the physics of dense plasmas. Nevertheless, follow-up ground-based observations, theoretical improvements and advanced classification meth-

ods (Torres et al. 1998; García-Berro et al. 2003a) will be needed in order to analyze the disk and halo populations.

Acknowledgements. Part of this work was supported by the MCYT grants AYA04094-C03-01 and 02, by the European Union FEDER funds, and by the CIRIT. L.G. Althaus is gratefully acknowledged for stimulating discussions and for providing the cooling sequences necessary for computing the disk white dwarf luminosity functions of Fig. 8. We also acknowledge our referee, Chris Flynn, for a very careful reading of the original manuscript and for his valuable and constructive criticisms and comments.

REFERENCES

- Adams, F.C., & Laughlin, G., 1996, *ApJ*, 468, 586
- Alcock, C., Allsman, R.A., Axelrod, T.S., Bennett, D.P., Cook, K.H., Freeman, K.C., Griest, K., Guern, J.A., Lehner, M.J., Marshall, S.L., Park, H.-S., Perlmutter, S., Peterson, B.A., Pratt, M.R., Quinn, P.J., Rodgers, A.W., Stubbs, C.W., Sutherland, W., 1996, *ApJ*, 461, 84
- Alcock, C., Allsman, R.A., Alves, D.R., Axelrod, T.S., Becker, A.C., Bennett, D.P., Cook, K.H., Dalal, N., Drake, A.J., Freeman, K.C., Geha, M., Griest, K., Lehner, M.J., Marshall, S.L., Minniti, D., Nelson, C.A., Peterson, B.A., Popowski, P., Pratt, M.R., Quinn, P.J., Stubbs, C.W., Sutherland, W., Tomaney, A.B., Vandehei, T., & Welch, D., 2000, *ApJ*, 542, 281
- Benvenuto, O.G., & Althaus, L.G., 1999, *MNRAS*, 303, 30
- Binney, J., & Tremaine, H., 1987, *Galactic Dynamics* (Princeton Univ. Press: Princeton)
- Dehnen, W., & Binney, J.J., 1997, *MNRAS*, 287, L5
- Díaz-Pinto, A., García-Berro, E., Hernanz, M., Isern, J., & Mochkovitch, R., 1994, *A&A*, 282, 86
- García-Berro, E., Hernanz, M., Mochkovitch, R., & Isern, J., 1988, *A&A*, 193, 141
- García-Berro, E., Hernanz, M., Isern, J., & Mochkovitch, R., 1995, *MNRAS*, 277, 801
- García-Berro, E., Torres, S., Isern, J., & Burkert, A., 1999, *MNRAS*, 302, 173
- García-Berro, E., Torres, S., & Isern, J., 2003a, *Neural Networks*, 16, 405
- García-Berro, E., Torres, S., & Isern, J., 2003b, in *White Dwarfs*, Eds.: D. de Martino, R. Silvotti, J.E. Solheim & R. Kalytis, NATO Science Series (Kluwer Academic Publishers: Dordrecht) vol. 105, 23
- García-Berro, E., Torres, S., Isern, J., & Burkert, A., 2004, *A&A*, 418, 53
- Hakkila, J., Myers, J.M., Stidham, B.J., Hartmann, D.H., 1997, *AJ*, 114, 2043
- Hansen, B.M.S., & Liebert, J.W., 2003, *Ann. Rev. A&A*, 41, 465
- Hernanz, M., García-Berro, E., Isern, J., Mochkovitch, R., Segretain, L., & Chabrier, G., 1994, *ApJ*, 434, 652
- Hollik, W., 1997, *J. Phys. G: Nucl. Part. Phys.*, 23, 1503
- Iben, I. Jr., Laughlin, G., 1989, *ApJ*, 341, 312
- Isern, J., García-Berro, E., Hernanz, M., Mochkovitch, R., & Burkert, A., 1995, in *White Dwarfs*, Eds.: D. Koester & K. Werner (Berlin: Springer Verlag), 19
- Isern, J., Mochkovitch, R., García-Berro, E., & Hernanz, M., 1997, *ApJ*, 485, 308
- Isern, J., García-Berro, E., Hernanz, M., Mochkovitch, R., & Torres, S., 1998a, *ApJ*, 503,
- Isern, J., García-Berro, E., Hernanz, M., & Mochkovitch, R., 1998b, *Jour. of Phys.: Condensed Matter*, 10, 11263
- Isern, J., Hernanz, M., García-Berro, E., & Mochkovitch, R., 1999, in *Proc. of the 11th Workshop on White Dwarfs*, ASP Conf. Ser., vol. 169, Eds.: J.E. Solheim & E.G. Meistas (ASP: San Francisco), 408
- Isern, J., García-Berro, E., & Salaris, M., 2001, in *Astrophysical Ages and Timescales*, ASP Conf. Ser., vol. 245, Eds.: T. von Hippel, C. Simpson & N. Manset (ASP: San Francisco), 328
- Isern, J., & García-Berro, E., 2004, in *Lecture Notes and Essays in Astrophysics I*, Eds.: A. Ulla & M. Manteiga (Publications of the RSEF: Vigo), 23, <http://www.slac.stanford.edu/econf/C0307073>
- James, F., 1990, *Comput. Phys. Commun.*, 60, 329
- Koester, D., 2002, *A&A Rev.*, 11, 33
- Lasserre, T., Afonso, C., Albert, J.N., Andersen, J., Ansari, R., Aubourg, É., Bareyre, P., Bauer, F., Beaulieu, J.P., Blanc, G., Bouquet, A., Char, S., Charlot, X., Couchot, F., Coutures, C., Derue, F., Ferlet, R., Glicenstein, J.F., Goldman, B., Gould, A., Graff, D., Gros, M., Haissinski, J., Hamilton, J.C., Hardin, D., de Kat, J., Kim, A., Lesquoy, É., Loup, C., Magneville, C., Mansoux, B., Marquette, J.B., Maurice, É., Milsztajn, A., Moniez, M., Palanque-Delabrouille, N., Perdureau, O., Prévot, L., Regnault, N., Rich, J., Spiro, M., Vidal-Madjar, A., Vigroux, L., & Zylberajch, S., 2001, *A&A*, 355, L39
- Lorén-Aguilar, P., García-Berro, E., Isern, J., & Kubyshein, Y.A., *Class. & Quantum Grav.*, 20, 3885
- Marković, D., & Sommer-Larsen, J., 1997, *MNRAS*, 288, 733
- Mihalas, D., & Binney, J., 1981, *Galactic Astronomy* (W.H. Freeman & Co.: New York)
- Noh, H.-R., & Scalo, J., 1990, *ApJ*, 352, 605
- Ogorodnikov, K.F., 1965, *Dynamics of Stellar Systems* (Pergamon Press: New York)
- Oswalt, T.D., Smith, J.A., Wood, M.A., & Hintzen, P., 1996, *Nature*, 382, 692
- Perryman, M.A.C., 2002, in *EAS Pub. Ser., Vol. 2, Proc. of GAIA: A European Space Project* (EDP Sciences: Les Ulis, France)
- Perryman, M.A.C., de Boer, K.S., Gilmore, G., Hoeg, E., Lattanzi, M.G., Lindegren, L., Luri, X., Mignard, F., Pace, O., de Zeeuw, P.T., 2001, *A&A*, 369, 339
- Press, W.H., Flannery, B.P., Teukolsky, S.A., Vetterling, W.T., 1986, *Numerical Recipes* (Cambridge Univ. Press; Cambridge, UK)
- Richer, H.B., Hansen, B., Limongi, M., Chieffi, A., Straniero, O., & Fahlman, G.G., 2000, *ApJ*, 529, 318
- Salaris, M., Domínguez, I., García-Berro, E., Hernanz, M., Isern, J., & Mochkovitch, R., 1997, *ApJ*, 486, 413
- Salaris, M., García-Berro, E., Hernanz, M., Isern, J. & Saumon, D., 2000, *ApJ*, 544, 1036
- Salim, S., & Gould, A., 2003, *ApJ*, 582, 1011
- Scalo, J., 1998, in *The Stellar Initial Mass Function*, Eds.: G. Gilmore & D. Howell (PASP Conference Series: San Francisco), Vol. 142, 201
- Schmidt, M., 1968, *ApJ*, 151, 393
- Torres, S., García-Berro, E., & Isern, J., 1998, *ApJ*, 508, L71
- Torres, S., García-Berro, E., Burkert, A., & Isern, J., 2001, *MNRAS*, 328, 492
- Torres, S., García-Berro, E., Burkert, A., & Isern, J., 2002, *MNRAS*, 336, 971
- Winget, D.E., Hansen, C.J., Liebert, J., van Horn, H.M., Fontaine, G., Nather, R.E., Kepler, S.O., & Lamb, D.Q., 1987, *ApJ*, 315, L77